

# Agricultural Robotic Platform with Four Wheel Steering for Weed Detection

Thomas Bak; Hans Jakobsen

Department of Agricultural Engineering, Danish Institute of Agricultural Sciences, Schöttesvej 17, DK-8700 Horsens, Denmark;  
e-mail of corresponding author: [tb@control.auc.dk](mailto:tb@control.auc.dk)

(Received 10 January 2003; accepted in revised form 14 October 2003; Published online 23 December 2003)

A robotic platform for mapping of weed populations in fields was used to demonstrate intelligent concepts for autonomous vehicles in agriculture which may eventually result in a new sustainable model for developed agriculture. The vehicle presented here is adapted to operate in 0.25 and 0.5 m row crops and equipped with cameras for row guidance and weed detection. A modular approach is taken with four identical wheel modules, allowing four wheel steering and propulsion of the platform. The result is improved mobility which allows parallel displacement of the vehicle during turns by decoupling adjustments in position from adjustments in orientation. Control of the platform is provided through a vehicle electronics and control system based on embedded controllers and standard communication protocols. The software implements a hybrid deliberate software architecture that allows a hierarchical decomposition of the operation. The lowest level implements a reactive feedback control mechanism based on an extension of simple control for car-like vehicles to the four wheel case. The controller design forces the front and rear of the vehicle to follow a pre-determined path and allows the vehicle to maintain a fixed orientation relative to the path. The controller rationale is outlined and results from experiments in the field are presented.

© 2003 Silsoe Research Institute. All rights reserved

Published by Elsevier Ltd

## 1. Introduction

Advances in mechanical design capabilities, sensing technologies, electronics, and algorithms for planning and control have led to a possibility of realising field operations based on autonomous robotic platforms. The need for such systems is driven by increasing financial pressure on farmers combined with public concern about the environment and working conditions. Efficient deployment of autonomous robotic platforms in the field will allow care and management of crops in a very different way from what is known today (Blasco *et al.*, 2002; Cho *et al.*, 2002). Robotic platforms and implements may sense and manipulate the crop and its environment in a precise manner with minimal amount of materials and energy making them potentially more efficient than traditional machinery. This is likely to reduce the environmental impact while increasing precision and efficiency (Kondo & Ting, 1998; De Baerdemaeker *et al.*, 2001). The result is a new sustainable model for developed agriculture.

Guidance of agricultural vehicles has been an active area of research for a number of years and the first commercial guidance systems for tractors are available. The tractors are guided along a pre-defined path primarily based on input from the global positioning system (GPS), alternatively the vehicles are operated relative to the crop line using machine vision (Tillett, 1991; Jahns, 2000). These automatically guided machines address some of the problems outlined above, but are not necessarily the best solution in terms of soil compaction, energy use, emission and precision.

Focusing on machinery that can operate continuously with minimal or no operator assistance allows us to think in terms of smaller, more specialised, machines built for precision and materials efficiency. Such vehicles will be able to work longer hours at a slower rate, giving the same, or even greater, overall output as conventional systems while minimising the problems with conventional machines as outlined above. The development of such robotic platforms that can operate in a biologically variable environment for longer periods of time with minimal human assistance is a major challenge. Recent

Notation			
$d_r$	perpendicular distance of rear steering point to path, m	$\gamma_f$	commanded direction of front steering point relative to vehicle, rad
$h$	velocity conversion factor, $V$ per $\text{m s}^{-1}$	$\gamma_r$	commanded direction of rear steering point relative to vehicle, rad
$k_p$	gain, steering direction control	$\delta_i$	distance from contact point $i$ to instantaneous centre of rotation, m
$K_1$	motor constant, ratio of change in torque to change in voltage, $\text{N m V}^{-1}$	$\delta_p$	distance from reference point $P$ to instantaneous centre of rotation, m
$K_2$	motor constant, ratio of change in torque to a change in speed, $\text{N m per rad s}^{-1}$	$\theta$	orientation of vehicle frame relative to reference frame, rad
$v_i$	velocity of wheel contact points, $\text{m s}^{-1}$	$\theta_{ef}$	orientation error relative to desired path tracked by front steering point, rad
$v_{cmd}$	commanded velocity, $\text{m s}^{-1}$	$\theta_{er}$	orientation error relative to desired path tracked by rear steering point, rad
$V_i$	motor voltage for motor $i$ , V	$\tau_i$	torque from motor $i$ , N
$x, y$	location coordinates of vehicle frame relative to reference frame, m	$\omega_i$	rotational velocity of motor shaft $i$ , $\text{rad s}^{-1}$
$x_{ICR}, y_{ICR}$	location coordinates of instantaneous centre of rotation relative to reference frame, m		

contributions in the area of robotics in the agricultural application domain are given in Baerveldt (2002) and in Torii (2000).

This paper discusses a specific robotic platform for mapping weed populations. The platform is the result of an ongoing research project which aims at demonstrating intelligent concepts for autonomous vehicles in agriculture. The design is adapted to operate in 0.25 and 0.5 m row crops. Guiding the vehicle relative to the crop lines using a row guidance camera optimises work rates, provides valuable localisation input, while minimising damage to the crops. Four wheel steering (4WS) was introduced to provide a flexible platform for the research, but the improved mobility also provides a number of more practical benefits. The 4WS allows parallel displacement of the vehicle during turns by decoupling adjustments in position from adjustments in orientation. It allows both the front and rear of the vehicle to follow a specific path precisely and implements such as weed mapping camera, sowing machine, hoe, *etc.* may maintain a fixed orientation relative to the crop rows. By parallel displacement of the vehicle, the traditional three-point turn may completely be eliminated. Steering on all wheels also minimises side slip of the wheels resulting in reduced wear on the vehicle and less damage to the field.

Given the non-linear nature of the vehicle with four independently controlled wheels the control problem is not trivial. However, with a relative low speed (maximum  $2\text{--}6 \text{ km h}^{-1}$ ), simple controllers can give good results. One approach that has been used with success, is a proportional controller on a point ahead of the vehicle (Billingsley & Shoenfish, 1995; Gerrish *et al.*, 1997; Wallace *et al.*, 1985). All these results address

conventional car-like vehicles with steering on two wheels, while fuzzy control of a 4WS vehicle is discussed in Toda *et al.* (1999). The approach taken here builds on the good experience with simple controllers for two wheel steering and introduces a simple way of extending that to the 4WS case. The result is a control strategy that avoids much of the complexity in traditional 4WS while maintaining certain desirable operational characteristics of the 4WS. The concept has been tested under realistic conditions in the field and all results presented here are from field tests.

This paper presents an overview of the system and approach. Section 2 provides a system description. This includes a description of a modular mechanical concept as well as the mechatronic implementation of the system. Everything is tied together in a hierarchical hybrid software architecture. In Section 3, the focus is on a specific mobility control strategy that extends simple controllers to 4WS. The result is a system that allows the vehicle to track a given path, while maintaining the front and rear implement bars on the path. Results from experiments in the field are summarised in Section 4 and demonstrate the effectiveness of the proposed 4WS solution. Finally, conclusions are drawn and discuss further research. This paper concentrates on the engineering aspects of the research and evaluation of the experimental system.

## 2. System description

The robotic platform described here is meant to demonstrate novel sensing capabilities (Søgaard & Olsen, 2000) and semi-autonomous operation of a

robotic platform for agriculture. The immediate agronomic aim of the project is to demonstrate efficient measurement of spatial and temporal crop and weed measurements. Given that the variability in weeds is measured and mapped, inputs can be varied according to a defined strategy providing environmental and economic benefits. Studies show that 50–80% of the costs for herbicides can be saved when treating only patches where weeds actually grow (Green *et al.*, 1997; Nordmeyer *et al.*, 1997). Fundamental for the success of such a system is the integration into farm management systems, *e.g.* job creation and path planning (Sørensen *et al.*, 2002).

The system consists of three principal components, a station or operating console, *e.g.* placed inside a tractor, a robotic platform and finally an implement which is responsible for the agronomic operation to be carried out. The station is responsible for communication with farm management and for global planning, while the platform implements movement according to a route computed by the station and collision avoidance. Communication between station and platform is based on a wireless network. The vision is to have a single operator supervising the robotic platform (or a fleet of platforms) while possibly performing other tasks in the field. The flexible platform supports different implements.

### 2.1. Robotic platform

The basis for the robotic platform is the mobility capability provided by the wheel module mechanism shown in *Fig. 1*. Each of the four identical wheel

modules include a brushless electric motor for propulsion that provide direct drive without gearing. Motor, amplifier and microcontroller are all mounted in the wheel hub. Steering capability is achieved by a separate steering motor mounted on top of the wheel module shaft to create a two-degree-of-freedom mechanism. The steering motor amplifier and the control electronics are mounted next to the steering motor. The control electronics (wheel node) are based on a commercial agricultural job computer and handle the local position servo control for the steering and provide torque control of the drive motors. The driver motor electronics allow speed and current (torque) feedback while the steering servo system provide a steering angle feedback derived from motor shaft encoders.

The wheel module has a simple mechanical interface that allows it to be mounted on virtually any vehicle chassis. The electrical interface includes a power interface (12–36 V) and a single controller area network (CAN) bus interface for controlling the module, *i.e.* the steering as well as the propulsion. The four identical wheel modules are attached to a 1.2 m by 1 m aluminium chassis resulting in a modular robotic platform as illustrated in *Fig. 2*.

The platform was designed specifically for agricultural use in rowcrops with good ground clearance (0.5 m), slim wheels and a 1 m wheel separation for in-row driving in 0.25 m rows. Passive stability is achieved by a three-point suspension system, that guarantees that all wheels are in contact with the ground. The platform provides a watertight front compartment for vehicle electronics, and a rear compartment for batteries and a possible user interface. Experiments and/or implements

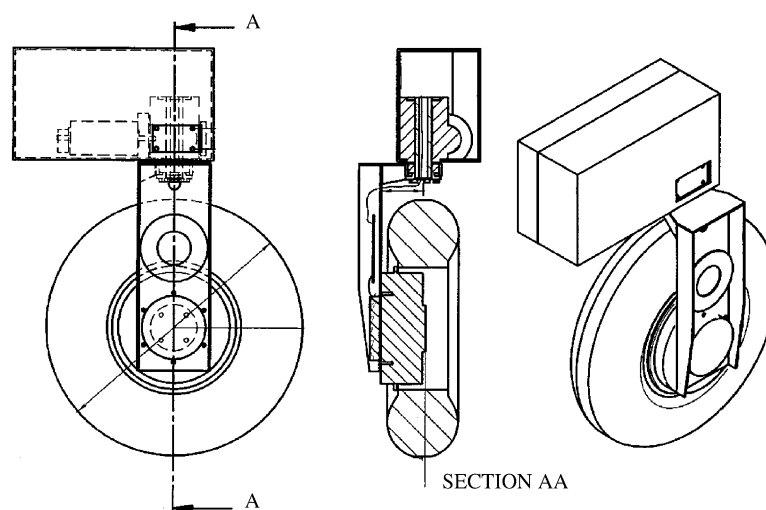


*Fig. 1. Wheel module: brushless hub wheel electric motors provide propulsion; steering is achieved by servo motors in the wheel module; the wheel module includes power and local velocity control for both steering and propulsion*

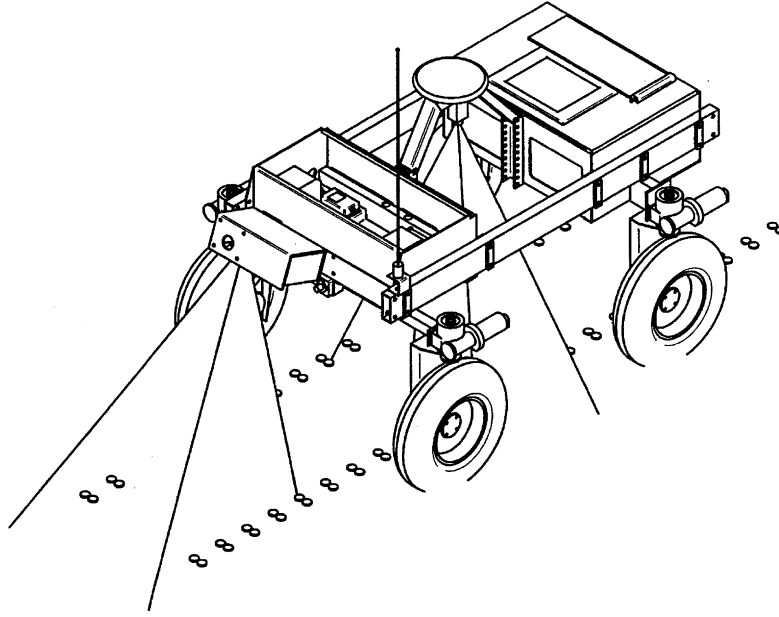


*Fig. 2. Schematic model of the experimental platform: vehicle localisation is achieved using a global positioning system, gyroscope, encoders and a row guidance camera; control is based on four wheel drive and four wheel steering; the total weight of the vehicle is 150 kg*

may be mounted at the centre of the platform, underneath the chassis or at the front- and rear-end implement bars.

## 2.2. Platform electronics

Control of the platform is provided through a mechatronic system that includes the mechanical concept just described and vehicle electronics and control systems to properly actuate the mechanical subsystem. The electronics architecture is built around a platform computer (PC/104 system) as shown in *Fig. 3*. The platform computer takes the central role in the control of the vehicle as it handles real-time vehicle control, sensor integration, and communication. The platform computer software is implemented on a Linux operating system. The development is supported by Mathworks real-time workshop (RTW), which allows generation of customisable C code directly from simulation models. This allows programs to be built automatically and subsequently execute in near real-time on the platform computer. The solution supports transmission control protocol/internet protocol (TCP/IP) sockets for remote communication with the running code which allows monitoring and modification of parameters during development.

Localisation is achieved by a redundant set of sensors that are interfaced to the platform computer using the RS232 serial communication protocol as well as a CAN

2-0b protocol. The primary navigation sensor is a Topcon Legacy dual frequency carrier phase differential GPS receiver capable of better than 2 cm standard deviation absolute accuracy. A KVH E-Core 2000 fibre-optic gyroscope precisely measures the heading rate. The gyroscope drift is controlled by including measurements from a magnetometer and wheel and steering encoders. By combining the reliability of the encoders, magnetometer and gyroscope, with the absolute position and accuracy of the GPS system, the platform position estimation process is robust to periodic GPS dropouts. The only absolute reference on heading is the magnetometer, but the plan is to include the row guidance camera in the fusion process to offset problems with the sensitivity of the magnetic measurements. The row guidance system is already mounted at the front implements toolbar and provides an angular reference relative to the plant rows. Actuation is provided by the four wheel modules. Each of the four modules provide local servo control of the drive motor torques and steering angles. The wheel node electronics are connected to the platform computer using a CAN 2-0b connection. Communication with experiments (and implements) electronics is achieved by a TCP/IP client server structure. The platform computer is a server that allows several clients (implements) to be connected. Alternatively implements may be connected via a second CAN bus connection that is available on the platform computer. Planning and monitoring take place in the station computer (console), which is accessible through

a wireless communication channel (wireless local area network).

### 2.3. System architecture

The system architecture adopted is similar to the hybrid deliberate approach (Arkin, 1990) that is now common in mobile robotics systems (Oreback & Christensen 2003). The three-layer architecture consists of: (1) a reactive feedback control mechanism that handles stabilisation and tracking, (2) a plan-execution

mechanism that deals with *e.g.* trajectory generation and task decomposition, and (3) a mechanism for performing time-consuming deliberative computations and interaction with human operators, *i.e.* job creation. The hierarchical structure is shown in Fig. 4.

The lowest level in the architecture handles reactive algorithms with hard real time bound on execution time. Some of the controllers at this level (*i.e.* the steering servo loops) have a high coupling with sensors and actuators and are situated in the wheel nodes, while *e.g.* the path tracking controller is situated in the platform computer. The path tracking requires a pose estimate,

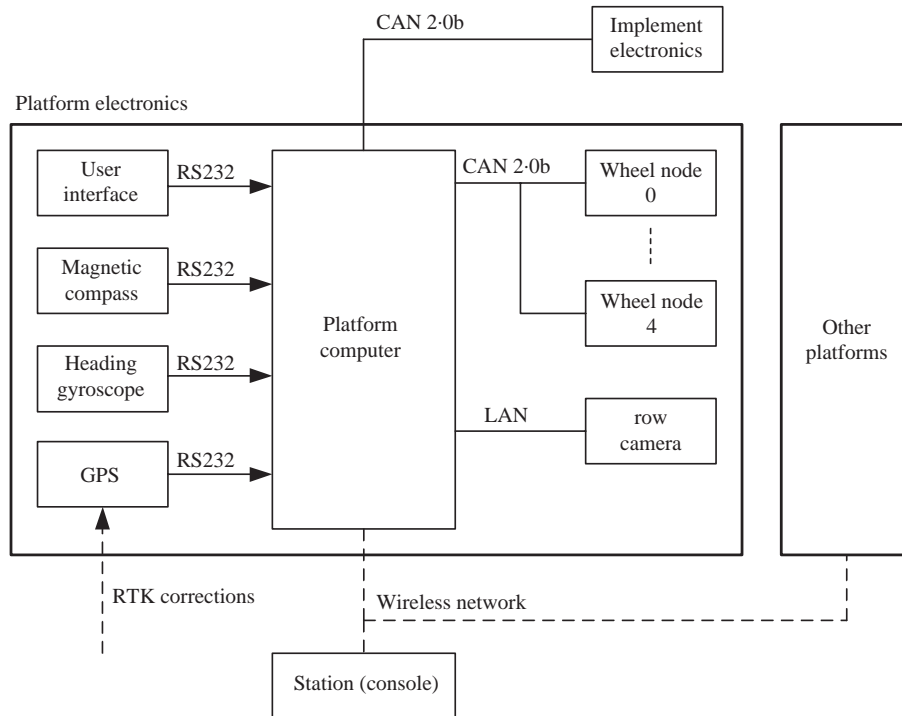


Fig. 3. Vehicle electronics: the platform computer communicates with sensors and actuators via controller area network (CAN) 2-0b, RS232 protocols, and local area network (LAN); a global positioning system (GPS) receiver provides positioning knowledge based on real time kinematic (RTK) corrections from a GPS base

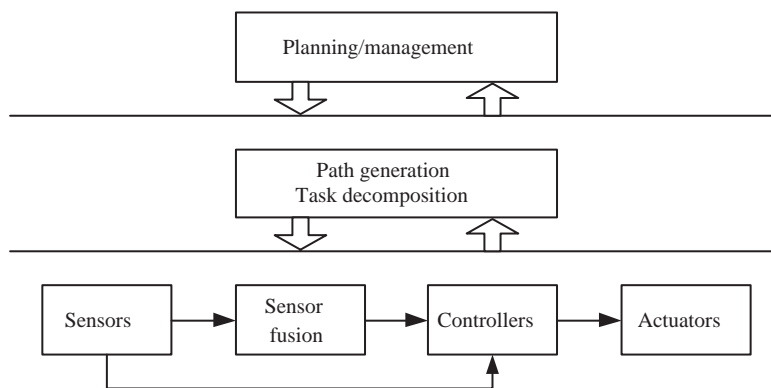


Fig. 4. The vehicle software architecture

which is extracted from the sensors by the sensor fusion module. The second level provides an abstraction from the concrete control algorithms. This allows a representation of the tasks performed by the controllers in terms of discrete states. This level of the architecture also defines the path segments that define the motion of the robot. The information passed to the controllers from the intermediate level takes the form of commands that encode desired vehicle behaviour (*e.g.* translate, follow path without rotating) as well as the desired path. Discussion of work related to the discrete mechanisms is presented by Bak *et al.* (2003). Information passed back to the plan-execution mechanism includes vehicle status information (position, orientation) and information regarding obstacles. Finally the planning/management module, situated at the station allows interfacing with farm management systems and users. It provides objectives for the operation of the vehicle. In the current system, the functionality of the management system includes the planning of the observation operation. It determines sampling points to be visited by the robotic platform in order to perform a mapping of the field in terms of weed densities. The sampling scheme is based on strategic planning (based on previous knowledge on the weed population in the field) and adaptive planning to allow dynamic replanning of the path according to unexpected occurrence of weed in the field (Sørensen *et al.*, 2002).

### 3. Mobility control

The motion of the robot can always be viewed as an instantaneous rotation around a time varying point called the instantaneous centre of rotation (ICR). Hence, at each instant, the velocity vector of any point of the frame is orthogonal to the straight line joining this point and the ICR.

Controlling the vehicle position in the field implies controlling the two-dimensional location of the ICR, which may be achieved by specifying the direction of travel of two points of the vehicle. To get experimental results with the 4WS system, a simple controller that controls two steering points was implemented, one at the front end and one at the rear of the vehicle. The 4WS is then utilised to minimise the distance to the desired path for both steering points independently as indicated in Fig. 5.

This approach with two independent controllers allows us to switch between 2WS and 4WS without having to change the controller structure. As front and rear controllers are identical so without loss of generality, the description here is focused on the front steering controller. Its control objective is to minimise the

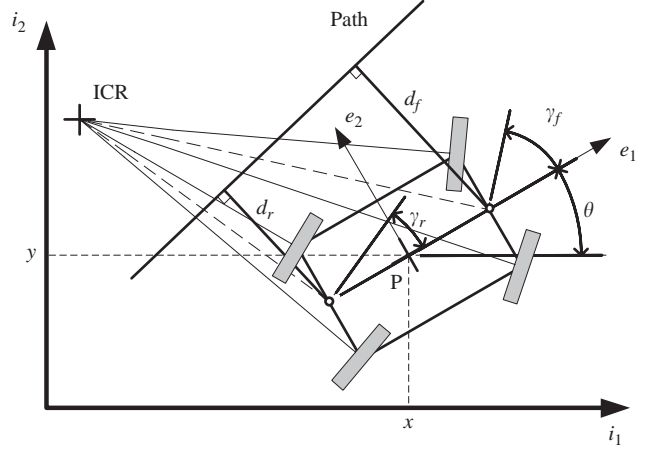


Fig. 5. The path following problem: the aim of the control is to minimise the distance of the front and rear steering points (indicated by circle) independently;  $d_f$  front and  $d_r$  rear steering point; instantaneous centre of rotation (ICR);  $e_1$ ,  $e_2$ , vehicle frame;  $P$  reference frame location;  $i_1$ ,  $i_2$ , reference frame;  $x$ ,  $y$  and  $\theta$ , vehicle pose;  $\gamma_f$ ,  $\gamma_r$ , commanded direction of travel of the front and rear steering point

perpendicular distance to the path  $d_f$ . The sign of  $d_f$  indicates the side of the path on which the steering point is located. From  $d_f$  it calculates a commanded direction of the front steering point (FSP) relative to the vehicle  $\gamma_f$ , using:

$$\gamma_f = \begin{cases} k_p d_f \pi / 2 - \theta_{ef} & \text{for } |d_f| \leq 1/k_p \\ \text{sign}(d_f) \pi / 2 - \theta_{ef} & \text{otherwise} \end{cases} \quad (1)$$

where:  $\theta_{ef}$  is the vehicle orientation relative to the path that the FSP is tracking (*i.e.* the orientation error); and  $k_p$  is the gain. The conditions on Eqn (1) ensure that the commanded angle relative to the path never exceeds  $\pm \pi/2$ . That is, when the distance exceeds  $1/k_p$  it moves straight towards (perpendicular to) the path. The rear steering point (RSP) has a  $\gamma_r$ , that is defined in a way similar to Eqn (1) using the errors in distance and angle associated with the RSP. Based on  $\gamma_f$  and  $\gamma_r$ , the location of the ICR in the vehicle frame may be found by geometry. The result is:

$$[x_{ICR} \ y_{ICR}]^T = \begin{cases} [10^7 \sin(\gamma_f) \ 10^7 \cos(\gamma_f)] & \text{if } \gamma_r = \gamma_f \\ [-0.51 / \tan(\gamma_f)] & \text{if } \gamma_r = 0 \\ \left[ \frac{0.5 + 0.5 \tan(\gamma_f) / \tan(\gamma_r)}{1 - \tan(\gamma_f) / \tan(\gamma_r)} \frac{0.5 - x_{ICR}}{\tan(\gamma_f)} \right] & \text{otherwise} \end{cases} \quad (2)$$

where:  $x$  and  $y$  are the location coordinates of the ICR in the plane; and  $T$  is the transpose operator. The conditions above handle singularities in the ICR solution. The next step is to transform the ICR location to wheel locations. The rotation of the wheels about the



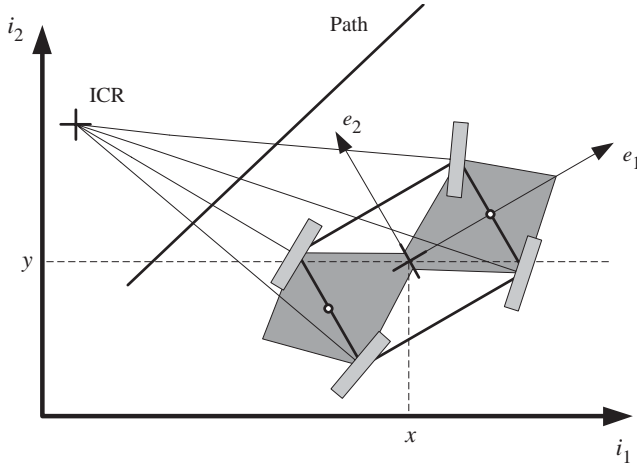


Fig. 6. Instantaneous centre of rotation (ICR) exclusion zones: the zones are established to avoid singular wheel configurations and to enforce limits on the steering angles; the vehicle rotates about the ICR;  $e_1$ ,  $e_2$ , vehicle frame;  $i_1$ ,  $i_2$ , reference frame;  $x$ ,  $y$ , position in reference frame

vertical axis is currently limited to  $\pm 135^\circ$  resulting in a constraint on the ICR location according to Fig. 6. If the ICR location is within the grey zone, it is transferred perpendicular to the edge. This simple solution guarantees that no singular configurations of the wheels are met, by limiting the ICR location we ensure that the feasible wheel configuration may be constructed.

The third degree of freedom is controlled using a proportional integral (PI) controller on the speed  $v_p$ . In order to achieve a desired vehicle speed while maintaining a pure rolling condition a torque distribution for the four wheels is established. The velocity of each of the four contact points of the wheels  $v_i$  is found from the following relationship:

$$v_i = \frac{\delta_i}{\delta_p} v_p \quad i = 1, \dots, 4 \quad (3)$$

where:  $\delta_i$  is the distance of contact point  $i$  to the ICR; and  $\delta_p$  is the distance from the reference point P in the vehicle frame to the ICR. The  $\delta_p$  singularity is avoided by the ICR limitations illustrated in Fig. 6. As a result the vehicle will not be able to perform pure rotation.

The output from the PI controller  $v_{cmd}$  is distributed as motor voltages  $V_i$  on each of the four motors by simply using a relationship similar to Eqn (3):

$$V_i = \frac{\delta_i}{\delta_p} h v_{cmd} \quad i = 1, \dots, 4 \quad (4)$$

where:  $h$  is a positive scalar converting the control signal to motor voltage.

In effect, this distribution makes the torques applied to each of the motors proportional to their distance to the ICR,  $\delta_i$ , as shown in Eqns (4) and (5). Using the

simplified DC motor equation:

$$\tau_i = K_1 V_i - K_2 \omega_i \quad i = 1, \dots, 4 \quad (5)$$

where:  $K_1$  and  $K_2$  are motor constants assumed identical for the four motors;  $\tau_i$  is the motor torque; and  $\omega_i$  is the angular velocity of the motor. Using that  $v_i = \omega_i r_i$  where  $r_i$  is the radius of wheel  $i$ , in combination with Eqn (3) we can estimate the electromotive force (EMF) and inserting the distribution from Eqn (3) results in:

$$\tau_i = \frac{\delta_i}{\delta_p} (K_1 h v_{cmd} - K_2 v_p / r_i) \quad i = 1, \dots, 4 \quad (6)$$

The part in the brackets is the same for all wheels if motors and wheel radius are identical. Therefore, the torque  $\tau_i$  is proportional with  $\delta_i$  and when turning, the outer wheel contributes with a larger torque than the inner wheels.

This simple distribution actually works very well in practice and in addition it also has an anti-spin effect. If a wheel slips, it will of course rotate a little faster as the EMF will grow to compensate for the missing torque, but the torque distribution among the wheels is not changed. A slipping wheel has a minor influence on the measured vehicle speed as it is based on the rotation speed of all wheels, but this can be solved by omitting a wheel if a slip detection indicates that it is slipping.

#### 4. Experimental results

In order to verify the overall concept of the platform and the control just outlined above a number of experiments have been carried out. An illustration of the vehicle during experiments is given in Fig. 7. The experiment is carried out in spring 2003. A path was pre-defined using a series of waypoints connected via straight line (path) segments. The result is a number of paths with relative sharp turns which indicated the efficiency of the proposed concept and control strategy. The sharp turns limits the potential forward velocity of the vehicle due to the limited steering motor response time. As indicated in Fig. 7, even a modest turn requires a significant response of the front wheels. Tests have shown the a response time of 800 ms on a  $70^\circ$  turn on the front wheels at only  $0.2 \text{ m s}^{-1}$ . Higher forward velocity is achievable only after a more sophisticated path generation. A tilt sensor built into the magnetometer is very sensitive to rough ground, the result being low performance in the estimation of orientation. The aim is to handle this problem in future experiment by including row guidance information as an orientation reference.

The following presents the results from an experiment where the vehicle is driving at  $0.4 \text{ m s}^{-1}$  with a short test

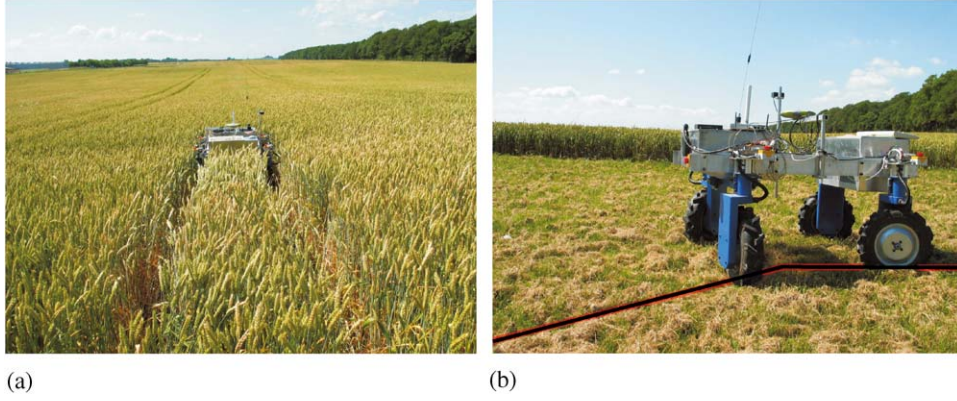


Fig. 7. The robotic platform in operation: (a) the vehicle travels along crop lines; (b) the vehicle follows a pre-defined path as indicated in the grass

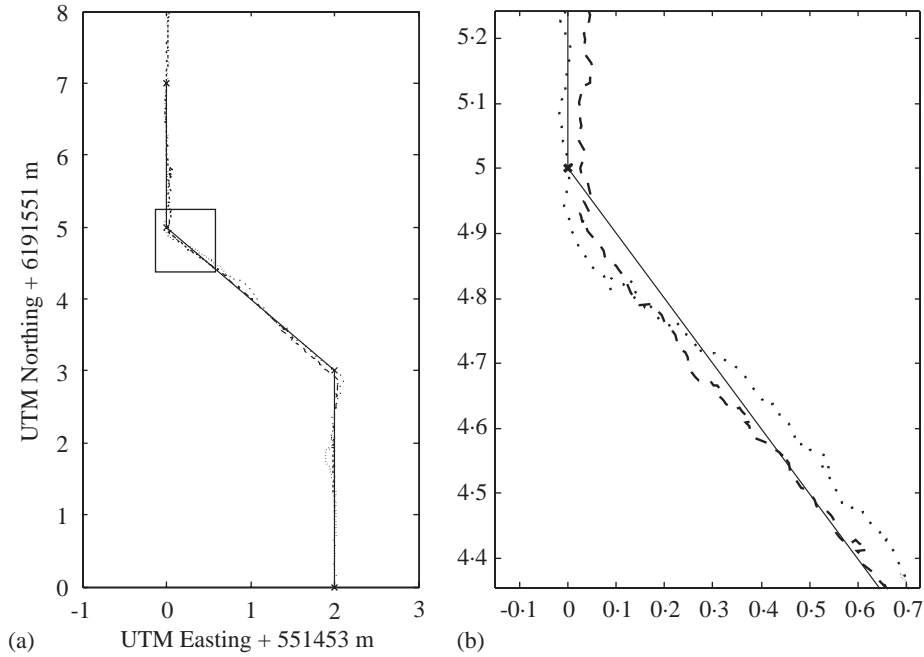


Fig. 8. Path following results with four wheel steering: (a) overview of row transition; (b) details of corner; Universal Transverse Mercator (UTM) coordinates;  $\times$ , waypoints;  $\cdots$ , position of front steering point;  $-$ , position of rear steering point

route containing two sharp turns, which causes it to make a 2 m sideways translation. The results from such an experiment are given in Fig. 9.

As the vehicle has 4WS the two steering points both follow the path closely. However, looking closer at one of the turns reveals some systematic errors. A presentation of the errors in terms of distance to path is given in Fig. 9.

When the FSP reaches the sharp turn, the RSP shows a systematic error towards east. This happens because the FSP moves in a different direction than the RSP, which introduces a ramp-like disturbance to the

orientation error of the RSP,  $\theta_{er}$ . The simple proportional controller in use cannot overcome a ramp input and thus there is a steady-state error. The FSP shows the same systematic error towards north east after having reached the sharp turn, because the RSP disturbs  $\theta_{ef}$ . This is, however, less clear from the figure because there is also a transient overshoot due to the finite turning velocity of the steering motors. The same systematic errors show up at the second sharp turn.

The errors would be removed with a better controller, but even with this controller the results are much better than a similar 2WS vehicle. In Fig. 10 the same steering



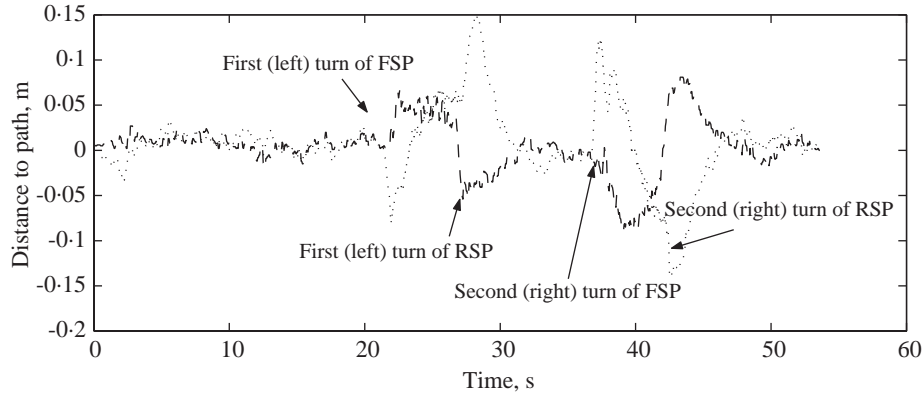


Fig. 9. Deviation from the desired path with four wheel steering: the distance from the two steering points to the path are plotted; FSP, front steering point, RSP, rear steering point;  $\cdots$ , position of front steering point;  $-$ , position of rear steering point

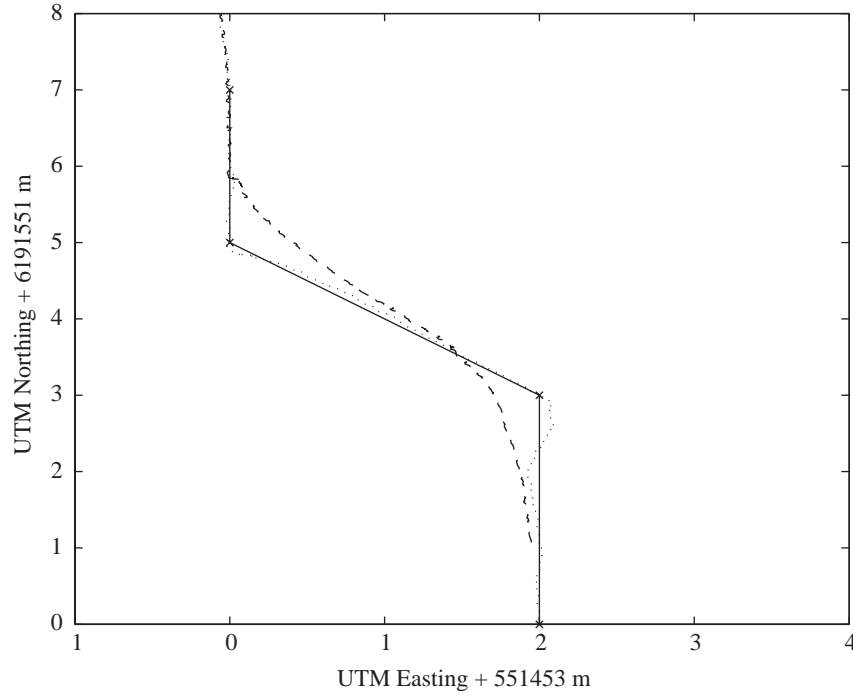


Fig. 10. Path following results with conventional front wheel steering: the distance from the two steering points to the path are plotted; Universal Transverse Mercator (UTM) coordinates;  $\times$ , waypoints;  $\cdots$ , position of front steering point;  $-$ , position of rear steering point

points are plotted for a test drive with a value for  $\gamma_r$  of 0. It is clear that the RSP cuts the corners, making it impossible to place implements requiring precision at the rear.

A comparison of the errors committed by the RSP using 4WS and a conventional front wheel steering is given in Fig. 11. It is clear that the excursions from the path by the 2WS vehicle are significantly larger. The large deviations in Fig. 11 are a result of the way the path is generated, by interconnecting waypoints using

straight lines. As the path tracking moves past the perpendicular to a path segment, the error jumps to the next segment, causing a jump in the error. This could be overcome with a fitting of the waypoints by *e.g.* monotone splines.

To better quantify the accuracy of the proposed solution two experiments were carried out with a series of 11 and 45° turns as indicated in Fig. 12. As indicated in Fig. 12(a), the vehicle travels at 0.2 m s<sup>-1</sup> and there is a separation of the turns of 5 m. The tracking accuracy

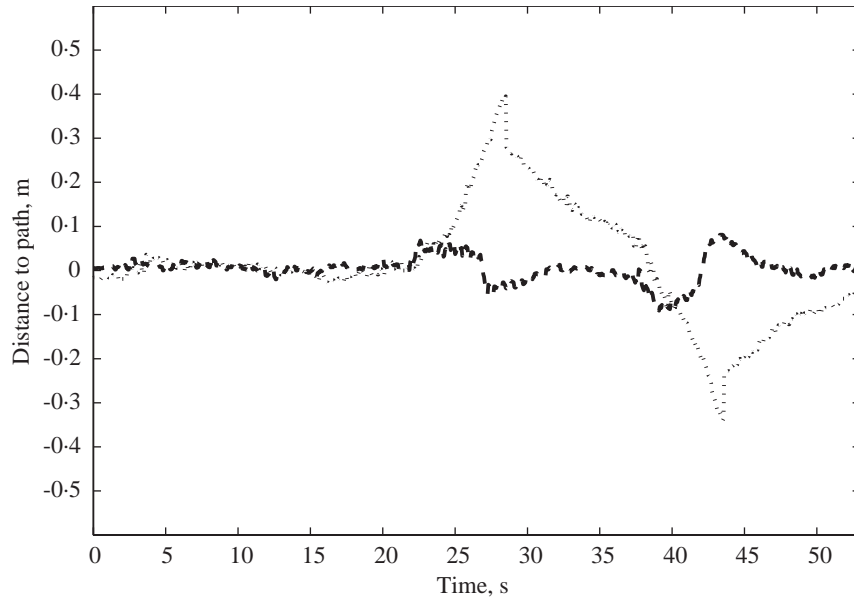


Fig. 11. Deviation from the desired path (rear steering point) using four wheel steering (4WS) and conventional two wheel front wheel steering (2WS): the significant changes at 28 s and 43 s appears as the robot initiates tracking of new path segments;  $\cdots$ , 2WS;  $--$ , 4WS

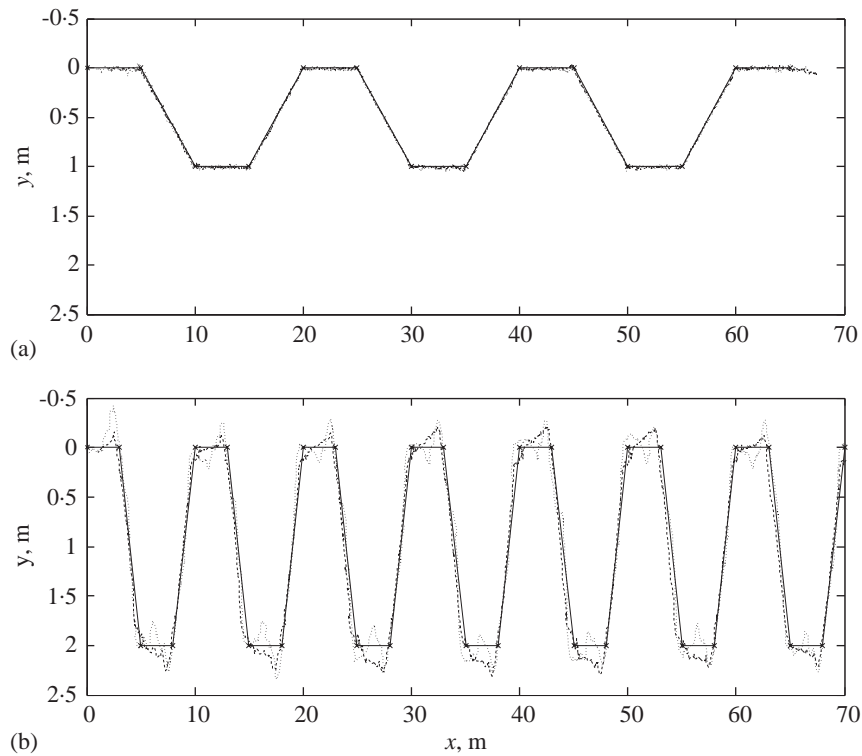


Fig. 12. Two test scenarios with multiple turns: (a) multiple  $11^\circ$  turns at  $0.2 \text{ m s}^{-1}$ , (b) multiple  $45^\circ$  turns at  $0.4 \text{ m s}^{-1}$ ;  $\times$ , waypoints;  $\cdots$ , actual path of vehicle;  $-$ , commanded path

of the FSP and RSP is 1.0 and 1.6 cm, respectively (1 sigma). At a higher forward velocity of  $1.6 \text{ m s}^{-1}$  the accuracy grows to 7.9 and 10.7 cm (1 sigma). In

Fig. 12(b), the vehicle travels at  $0.4 \text{ m s}^{-1}$  with  $45^\circ$  turns which introduces a significant error due to the limitation in the steering motor response.

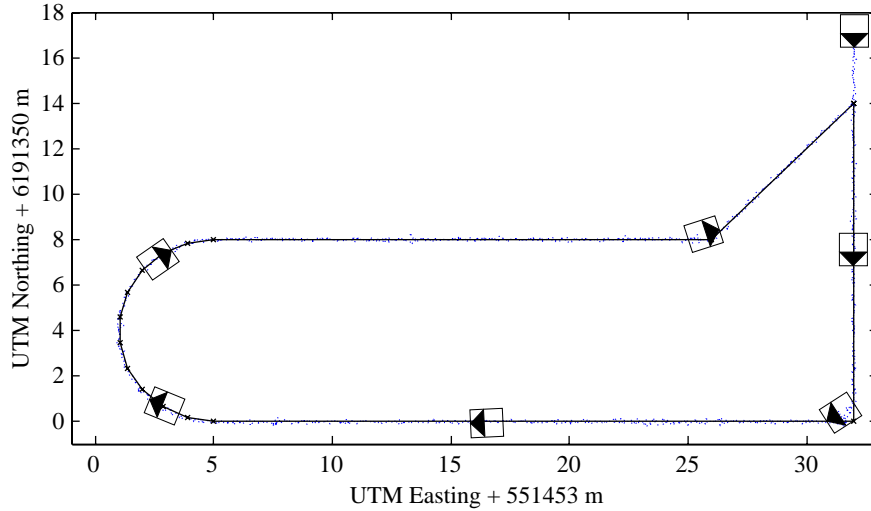


Fig. 13. Path tracking experiment: the vehicle follows a pre-defined path used in weed identification and mapping experiments; Universal Transverse Mercator (UTM) coordinates;  $\cdots$ , position of the front steering point;  $-$ , waypoint interpolation

More sophisticated manoeuvres have been carried out with the vehicle as illustrated in Fig. 13. Here the vehicle tracks a pre-defined path in the field (see Fig. 7). The vehicle starts at the position in the plane,  $(x, y) = (32, 16)$  m, tracks straight lines, performs a  $180^\circ$  turn along an arch and returns to the starting position.

The aim of the experiments outlined above has been to demonstrate an end-to-end test of the feasibility of our 4WS robotic platform. The figures only show the results in terms of path tracking, but doing so demonstrates that the platform can be localised using the available sensors, find the errors in pose relative to a path, apply simple control laws and communicate the corrections to the wheel modules for actuation. The experiments are, however, only the first step in establishing a truly autonomous platform.

## 5. Conclusion

This paper has described an autonomous vehicle with improved manoeuvrability in the field based on a four wheel steering (4WS) concept and a distributed, multi-processor control system. The robotic platform is based on a modular wheel concept that includes low level actuation, sensing and processing. The wheels are integrated with a chassis generating a flexible platform for experiments and implements. The instrumentation of the platform allows real time localisation and control. Motion of the platform is controlled via platform software that is based on a hybrid deliberate architecture that allows integration into farm management and planning systems. Given the non-linear nature of the

4WS path tracking problem, the control problem is not trivial. A simple solution that extends conventional two wheel steering to 4WS, is presented. At the relative low speed of the vehicle these solutions allow the tracking of a path while maintaining a fixed orientation relative to the path. Experiments have demonstrated the effectiveness of the 4WS based on a simple control strategy. The results indicate a  $1.0\text{--}1.6$  cm standard deviation on the path tracking for  $0.2\text{ m s}^{-1}$  forward velocity on a path with moderate turns. For a similar path the error grows to  $7.9\text{--}10.7$  with a velocity of  $1.6\text{ m s}^{-1}$ . While the sharp turns demonstrate the effectiveness of the proposed concept and control strategy they also reveal the limitation in the steering motor response time.

The results presented here are only the first step in demonstrating autonomous behaviour in the field. Our ongoing and future research considers the mobility advantages offered by the 4WS platform over more conventional systems and looks for more sophisticated ways to control the orientation and position independently by adding more control mechanisms to the reactive layer. This includes a hybrid system approach to the singularities in the wheel configurations and instantaneous centre of rotation (ICR) locations. This approach also addresses the problem of path generation by investigating it as a stability problem. Potentially many of the path problems may be overcome by simply using monotone splines combined with a stability proof.

A simple modification of the wheel modules, will allow the range on the steering wheels to be extended to  $\pm 180^\circ$  allowing positioning the ICR more freely. To achieve more robust performance of the localisation we are looking at ways to include row guidance system in

the sensor fusion solution. While focus here has been on the reactive behaviour of the path tracking control mechanism, research is also currently addressing the plan-execution mechanism and the deliberative computations in the planning/management interface.

### Acknowledgements

The work was supported by the Danish Ministry of Food, Agriculture and Fisheries under contract 93S-2466-A00-01367. Thanks to T.E. Madsen for providing the drawings of the vehicle structure and wheel module.

### References

- Arkin R C** (1980). Integrating behavioral, perceptual and world knowledge in reactive navigation. *Journal of Robotics and Autonomous Systems*, **6**, 105–122
- Baerveldt A-J** (2002). Guest Editorial: Special Issue on Agricultural Robotics. *Autonomous Robots*, **13**(1), 5–7
- Bak T; Bendtsen J; Ravn A P** (2003). Hybrid control design for a wheeled mobile robot. In: Springer-Verlag Lecture Notes in Computer Science, Vol. 2623 (Pnueli A; Maler O, eds), pp 50–65, Springer, Berlin
- Billingsley J; Shoenfish M** (1995). Vision guidance of agricultural vehicles. *Autonomous Robots*, **2**(1), 65–76
- Blasco J; Aleixos N; Roger J M; Rabatel G; Moltó E** (2002). Robotic weed control using machine vision. *Biosystems Engineering*, **83**(2), 149–157
- Cho S I; Chang S J; Kim Y Y; An K J** (2002). Development of a three-degrees-of-freedom robot for harvesting lettuce using machine vision and fuzzy logic control. *Biosystems Engineering*, **82**(2), 143–149
- De Baerdemaeker J; Munack A; Ramon H; Speckmann H** (2001). Mechatronic systems, communication, and control in precision agriculture. *IEEE Control Systems Magazine*, **21**(5), 48–70
- Gerrish J; Fehr B; Ee G V; Welch D** (1997). Self-steering tractor guided by computer vision. *Applied Engineering in Agriculture*, **13**(5), 559–563
- Green H M; Vencill W K; Kvein C K; Boydell B C; Pocknee S** (1997). Precision management of spatially variable weeds. BIOS Scientific Publishers Ltd., Oxford, UK, In: *Precision Agriculture*, Vol. II (Stafford J, ed.), pp 983–989
- Jahns G** (2000). Introduction. Special Issue on Navigating of Agricultural Field Machinery. *Computers and Electronics in Agriculture*, **25**(1–2), 1–2
- Kondo N; Ting K** (1998). Robotics for bioproduction systems. American Society of Agricultural Engineering, Publ. 05-98
- Nordmeyer H; Häusler A; Niemann P** (1997). Spatial variability in soil and crop. In: *Precision Agriculture*, Vol. I (Stafford J, ed.), pp 307–313, BIOS Scientific Publishers Ltd., Oxford, UK
- Orebäck A; Christensen H I** (2003). Evaluation of architectures for mobile robotics. *Autonomous Robots*, **14**(1), 33–49
- Søgaard H T; Olsen H J** (2000). A new method for determination of crop row position by computer vision. EurAgEng Paper No. 00-AE-016, AgEng 2000, Warwick, UK
- Sørensen C; Olsen H; Ravn A; Makowski** (2002). Planning and operation of an autonomous vehicle. Proceedings 2002 ASEA/CIGR XVth World Congress, ASAE Paper No. 02-1177
- Tillett N** (1991). Automatic guidance for agricultural field machines: a review. *Journal of Agricultural Engineering Research*, **50**, 167–187
- Toda M; Kitani O; Okamoto T; Torii T** (1999). Navigation method for a mobile robot via sonar-based crop row mapping and fuzzy logic control. *Journal of Agricultural Engineering Research*, **72**(4), 299–309, doi:10.1006/jaer.1998.0371
- Torii T** (2000). Research in autonomous agriculture vehicles in Japan. *Computers and Electronics in Agriculture*, **25**(1–2), 133–153
- Wallace R; Stentz A T; Thorpe C; Moravec H; Whittaker W R L; Kanade T** (1985). First results in robot road-following. Proceedings of the International Joint Conference on Artificial Intelligence, pp 1089–1095, Los Angeles, CA, USA